Available online at www.sciencedirect.com
ScienceDirect
Journal of Power Sources 173 (2007) 909–916
JOURNAL OF POWER SOURCES
www.elsevier.com/locate/jpowsour

Two-cell theory to measure membrane resistance based on proton flow: Theory development and experimental validation

Susanta K. Das *, K.J. Berry

Center for Fuel Cell Systems and Powertrain Integrations, Kettering University, 1700 West Third Avenue, Flint, MI 48504, USA

Received 6 July 2007; received in revised form 15 August 2007; accepted 16 August 2007
Available online 1 September 2007

Abstract

A two-cell theory is developed to measure proton exchange membrane (PEM) resistance to proton flow during conduction through a PEM fuel cell. The theoretical framework developed herein is based upon fundamental thermodynamic principles and engineering laws. We made appropriate corrections to develop the theoretical model previously proposed by Babu and Nair (B.V. Babu, N. Nair, J. Energy Edu. Sci. Technol. 13 (2004) 13–20) for measuring membrane resistance to the flow of protons, which is the only ion that travels from one electrode to the other through the membrane. A simple experimental set-up and procedure are also developed to validate the theoretical model predictions. A widely used commercial membrane (Nafion®) and several in-house membranes are examined to compare relative resistance among membranes. According to the theory, resistance of the proton exchange membrane is directly proportional to the time taken for a specific amount of protons to pass through the membrane. A second order differential equation describes the entire process. The results show that theoretical predictions are in excellent agreement with experimental observations. It is our speculation that the investigation results will open up a route to develop a simple device to measure resistance during membrane manufacturing since electrolyte resistance is one of the key performance drivers for the advancement of fuel cell technology.

Keywords: Proton exchange membrane; Electrolyte resistance; Two-cell theory; pH monitor; Fuel cell technology

1. Introduction

Environment pollution from fossil fuel combustion has resulted in health problems in many urban areas and also contributed significantly to the accumulation of atmospheric greenhouse gases, resulting in detrimental global climate changes. The increasing consumption of finite fossil fuel reserves is alarming and provides motivation to search for alternative fuels and energy sources for sustainable development and environmental protection. Fuel Cell (FC), an electrochemical device, having almost no emission except for water and heat as by-product, is a promising candidate for a potential alternative, renewable, clean and energy efficient power source. Among different types of fuel cells [2] – proton exchange membrane fuel cell (PEMFC) is a good candidate for providing an alternative and sustainable clean energy for remote power supplies, potable power devices, stationary power generations, automotive power systems and a wide range of transportation applications [3–4]. The commercial success of PEMFCs depends more on their cost effectiveness as compared to other energy conversion and power generation devices. Cost reduction of PEM fuel cells can be achieved by enhancing performance, i.e. achieving high-energy conversion efficiency and power density, and lowering material and fabrication costs.

In PEMFCs, a membrane (electrolyte) is required to separate the chemical reactions at the electro-catalytic porous anode and cathode electrodes [2]. Humidified hydrogen is usually fed at the anode and humidified air/oxygen is fed at the cathode. At the anode, hydrogen molecule splits into two protons and two electrons. The electrons are directed through an external circuit for useful electric work before they reach the cathode electrode for participating in the chemical reactions. The protons travel through the membrane by diffusion to the cathode for the electrochemical reactions to take place. Since the important ingredient of PEM fuel cells is protons which migrate through the membrane, a successful fuel cell membrane must allow protons to move freely at a minimum resistance. This requirement has led many researchers to focus on cation exchange membranes [5].

* Corresponding author. Tel.: +1 810 762 7833; fax: +1 810 762 7860.
E-mail address: sdas@kettering.edu (S.K. Das).

0378-7753/$ – see front matter © 2007 Elsevier B.V. All rights reserved.
doi:10.1016/j.jpowsour.2007.08.066

Nomenclature

C	concentration [mol m^{-3}]
L	length of the membrane [mm]
N	flux [mol cm^{-3} s]
r	total resistance [ohms]
R	membrane resistance [Ohms]
t	time [min]
T	total time [min]
w	weight of the membrane [g]
ξ	solution resistance [ohms]
τ	mass transfer coefficient

subscripts

a	acid cell
am	acid cell–membrane interface
f	final
mw	membrane–water cell interface
w	water cell

These membranes have fixed anionic charges which often permit easy proton transport. The most commonly used polymer has been a perfluorinated sulfonic acid membrane best known by its trade name Nafion® [6]. The wide acceptance of this polymer is due to its specific characteristics such as chemically stable hydrophobic matrix filled with hydrophilic sulfonic acid clusters [5–7]. However, it is important to ensure that the membrane resistance does not increase excessively with cell current, even at current densities as high as 3 A cm^{-2} [8].

A successful membrane must not only conduct protons, but also have minimum resistance to prevent ohmic losses as well as efficiently prevent fuel transport through it to minimize the fuel loss, best known as fuel cross-over [2]. One of the key performance drivers for PEM fuel cell is the resistance of the membrane [2]. Because electrolyte is the medium through which protons produced at one electrode migrate to the other electrode in order to complete the electric circuit. The passage of ions within a phase of finite resistance gives rise to a voltage loss referred to as ohmic polarization [2]. Regardless of whether one considers the membrane to be the solid polymer in a proton exchange membrane (PEM) fuel cell, a high-temperature ionically conductive oxide in a solid oxide fuel cell (SOFC) or an acid-soaked matrix in phosphoric acid fuel cell (PAFC), membrane resistance is an important metric for fuel cell performance [2–4]. This article illustrates the development of a theoretical framework to efficiently measure membrane resistance within a fuel cell based on rigorous science and engineering laws.

Various experimental techniques are used for measurement of membrane resistance [9–10], such as: (i) current interrupt (iR), (ii) AC resistance, (iii) electrochemical impedance spectroscopy (EIS), and (iv) high-frequency resistance (HFR). Unfortunately, membrane resistance cannot be measured directly by conventional DC methods when installed in a fuel cell, nor can DC methods isolate electrolyte resistance from polarization resistance [2]. The experimental methods mentioned above are not accurate enough with each having advantages and disadvantages [2,10] and also complicated to implement at the membrane manufacturing stage. This study, therefore, explores a simple equipment requirement and measurement technique supported by a rigorous theoretical model to measure the membrane resistance at the manufacturing level.

The membrane resistance is a particularly important measure of single fuel cell (or fuel cell stack) electrical performance since it quantifies internal cell losses. It is desirable to monitor membrane resistance during membrane development and manufacturing of fuel cell stacks because ohmic losses generate waste heat that must be removed from the fuel cell, resulting in a decrease in overall electrical efficiency. In addition, since the fuel cell current densities are quite high compared to other electrochemical processes, even a very low ohmic resistance (milliohm) has a significant effect on over all fuel cell efficiency [2]. The resistance offered to proton flow in a fuel cell is primarily due to the membrane [11]. Besides membrane, the electrode–membrane interface also has a contribution to the over all cell resistance. But compared to the membrane resistance to protons flow, the interface resistances are very negligible [2–4]. Hence, the main objective of this study is two-fold: (i) to develop a correct theoretical framework eliminating ambiguities in previous model [1] to measure the resistance of a proton exchange membrane based on proton flow, as it is the only ion that migrate from one electrode to the other, and (ii) to develop a cost effective simple equipment set-up for the accurate validation of the theoretical model by experiment. The organization of this paper is as follows: details of theoretical model development are discussed in Section 2, experimental set-up is addressed in Section 3, results and discussions are given in Section 4. Concluding remarks are finally presented in Section 5.

2. Theoretical model to measure membrane resistance based on proton flow

We use the profiles of protons flow between two cells to measure the resistance of proton exchange membrane. A schematic of protons flow profile through the proton exchange membrane in the conductivity cell (electrolyte phase) together with the concentration profiles of protons in the acid and water phases are presented in Fig. 1. To minimize the complexity of the mathematical model, we assume that the protons concentration gradient can be approximated by a single-step linear difference between the concentration at the cells and interfaces. Therefore, the molar flux of protons in the acid cell towards the membrane can be expressed as the mass transfer coefficient in the acid, τ_a, multiplied by the concentration gradient [12]:

$$N = \tau_a \nabla C_{ac}, \tag{1}$$

$$\Rightarrow N = \tau_{am}(C_a - C_{am}), \tag{2}$$

where

$$\nabla C_{ac} = \frac{(C_a - C_{am})}{\xi_a}, \tag{3}$$

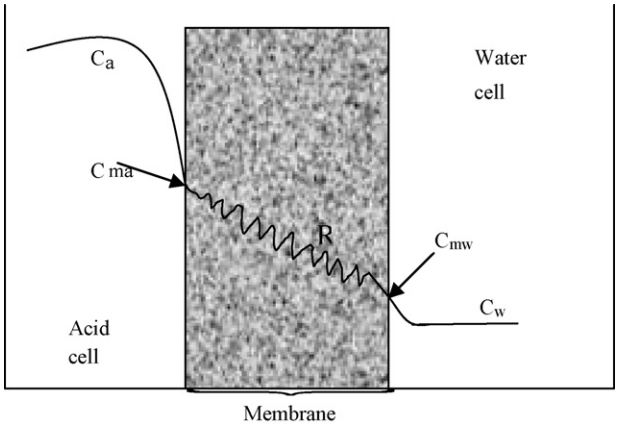

Fig. 1. Schematic of concentration profiles of protons in the acid and water cells. C_a is the proton concentration in bulk of acid phase, C_w is the proton concentration in bulk of water phase, C_{am} is the proton concentration on the interface of acid and membrane phase, C_{mw} is the proton concentration on the interface of membrane and water phase, R is the resistance of membrane to proton flow. All the concentrations, $C's$, vary with time.

$\tau_{am} = \tau_a/\xi_a$ denotes the modified mass transfer coefficient. Here, we considered solution resistance to protons flow in acid cell, ξ_a, for accurate calculation of resistance which was neglected in [1].

We further assume that the resistance offered to protons flow by the proton exchange membrane can be modeled as resistor, with resistance R, which has a potential difference of $(C_{am} - C_{mw})$ across the membrane (see Fig. 1). We assume that the number of protons leaving the acid cell per unit time equals the molar flux of protons through the membrane i.e. flow of protons satisfy the steady state condition. Thus, according to Ohm's law, $V = IR$, we obtain:

$$\mathrm{NR} = C_{am} - C_{mw}, \tag{4}$$

where the molar flux (proton flow – similar to electron flow), N, is analogous to the current flow.

Similarly for the water cell, we assume that there is no accumulation of protons in the membrane, i.e. the steady state condition is maintained, then we obtain:

$$N = \tau_w \nabla C_{wc}, \tag{5}$$

$$\Rightarrow N = \tau_{mw}(C_{mw} - C_w), \tag{6}$$

where

$$\nabla C_{wc} = \frac{(C_{mw} - C_w)}{\xi_w}, \tag{7}$$

τ_w is the mass transfer coefficient in water phase, $\tau_{mw} = \tau_w/\xi_w$ is the modified mass transfer coefficient between membrane–water interface and water phase, and ξ_w represents solution resistance to protons flow in water cell which was neglected in [1].

Adding Eqs. (2) and (6), we obtain

$$C_{am} - C_{mw} = (C_a - C_w) - N\left(\frac{1}{\tau_{am}} + \frac{1}{\tau_{mw}}\right), \tag{8}$$

where C_a and C_w are function of time.

Substituting Eq. (8) into Eq. (4), we get,

$$\mathrm{Nr} = (C_a - C_w), \tag{9}$$

where

$$r = \left(R + \frac{1}{\tau_{am}} + \frac{1}{\tau_{mw}}\right) \tag{10}$$

denotes the total effective resistance offered by the membrane, the acid-membrane and the water–membrane interfaces.

Since $C_a = C_a(t)$, we can write the molar flux of proton concentration in the acid cell as

$$N = -\frac{dC_a}{dt}. \tag{11}$$

As the steady-state condition is maintained throughout the systems, the rate of loss of protons from the acid cell must be equal to the rate of gain of protons in the water cell. Thus, we obtain,

$$-\frac{dC_a}{dt} = \frac{dC_w}{dt}. \tag{12}$$

Substituting Eq. (11) in Eq. (9) we get,

$$-r\frac{dC_a}{dt} = C_a - C_w. \tag{13}$$

Using Eq. (12), Eq. (13) can be written as

$$r\left(\frac{dC_w}{dt}\right) = C_a - C_w. \tag{14}$$

Differentiating Eq. (14) once with respect to time, t, we get:

$$r\frac{d^2C_w}{dt^2} = \frac{dC_a}{dt} - \frac{dC_w}{dt}. \tag{15}$$

Using Eq. (12), Eq. (15) can be reduced as:

$$\frac{d^2C_w}{dt^2} + \frac{2}{r}\frac{dC_w}{dt} = 0. \tag{16}$$

The Eq. (16) represents a second order ordinary differential equation which can be solved easily [13] for the proton concentration in the water cell, $C_w(t)$.

Let

$$C_w(t) = e^{qt} \tag{17}$$

be a trail solution [13] of Eq. (16) rather than the one assumed in [1]. Using Eq. (17), the general solution of Eq. (16) can be obtained as [13]:

$$C_w(t) = c_1 + c_2 e^{-(2/r)t}, \tag{18}$$

where c_1 and c_2 are the arbitrary constant, which can be determined from the limiting case.

Let the value of $C_w(t)$ at time $t = 0$ be C_0 and the value of $C_w(t)$ at time $t = \infty$ be C_f. The values of C_0 and C_f can be determined from the experiment. Substituting values of $C_w(0)$ and $C_w(\infty)$ in Eq. (18) we can find the values of c_1 and c_2. Thus, the final solution becomes

$$C_w(t) = C_f\left(1 - \left[\frac{C_f - C_0}{C_f}\right] e^{-t/(r/2)}\right). \tag{19}$$

Eq. (19) implies that the protons concentration in the water cell increases with time and attains its final value. The Eq. (19) can be written in a closed form as:

$$y = B(1 - Ae^{-t/\tau}), \tag{20}$$

where A, B are constants and $\tau = r/2$ serves as a time constant.

$$\text{At time } t = \frac{r}{2}, \tag{21}$$

from Eq. (19), we obtain:

$$C_w(t) = C_f\left(1 - 0.3679\left[\frac{C_f - C_0}{C_f}\right]\right). \tag{22}$$

The Eq. (22) is correctly derived and eliminated numerical error in Eq. (23) of reference [1]. The values of C_0 and C_f can be determined using a simple experiment described in the following section. In Eq. (22), the right hand side is completely known. Thus, the value of $C_w(t)$ can be easily found.

Using Eq. (22), the profiles of protons flow in the water cell, $C_w(t)$, can be plotted as a function of time, t, from which the value of t corresponding to the calculated value of $C_w(t)$ can be determined. Let the value of t be T. Hence, we obtain from Eq. (10) and (21):

$$r = \left(R + \frac{1}{\tau_{am}} + \frac{1}{\tau_{mw}}\right) = 2t = T, \tag{23}$$

where r has the units of time. Physical interpretation of Eq. (22) along with Eq. (23) is that to attain a particular value of $C_w(t)$ i.e. a specific amount of concentration of protons in the water cell, the total time required will be r. The greater the value of r, the longer time the membrane would take to allow those specific numbers of protons to pass into the water cell. It implies that r provides the measurement of the resistance of the membrane based on proton flow and r is directly proportional to the total time, T. Since the same experimental set-up and conditions are maintained in all the experiments to determine the values of C_0 and C_f, as required in Eq. (22), the value of $[(1/\tau_{am}) + (1/\tau_{mw})]$ remains constant throughout. Hence, the value of r depends only on R (according to Eq. (23)) i.e. the resistance of the membrane. In this simple way, we can measure the resistance offered to protons flow by each individual proton exchange membrane.

3. Experimental set-up and procedures

According to Eq. (22), to find the values of C_0 and C_f, which ultimately leads to the calculation of membrane resistance, R, the following experimental set-up and procedures are followed.

3.1. Set-up procedures

As shown in Fig. 2, the experimental set-up consists of two cells. The proton exchange membrane is placed in the PEM holder between the two cells. Silicone grease was applied around the outer edge of the PEM holder to ensure that transfer of protons from one cell to the other could not occur without passing through the PEM. First, same amount of de-ionized water was added to each cell. Then cells were allowed to equilibrate

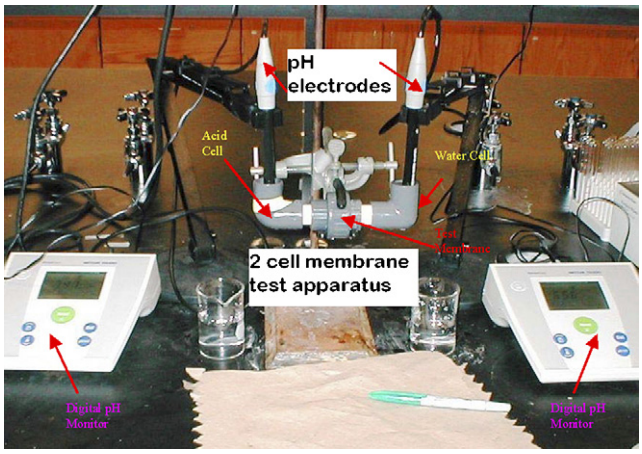

Fig. 2. Membrane resistance test apparatus: two-cell method. Acid cell, water cell and test membrane sections are labeled and indicated by arrow sign. pH meter is attached into each of the cells and pH is recorded at a regular time interval through the monitor.

so that the water on each side of the membrane achieved the same depth. A pH meter was fitted into each cell and a monitor connection with pH meter was then established within each cell on either side of the membrane to accurately record the pH readings. The pH meter must be quite accurate to detect small changes in the pH of the two cells. As soon as the pH meters have reached in equilibrium, few drops of de-ionized water were added to the left cell and few drops (number of drops are same for both cases) of concentrated HCl solution were added to the right cell simultaneously. This procedure ensures the volume of liquid in each cell remained the same so that there would be no liquid forced through the membrane by pressure difference (i.e. avoided pressure driven flow). In this way, we obtained, one acid cell containing concentrated HCl solution (20% HCl) and a water cell containing de-ionized water. The pH and temperature of both cells were recorded immediately. Since protons will move from the acid cell to the water cell there would be a negative gradient in the concentrations of protons. Thus, theoretically, protons must try to make their way across the membrane to migrate to the water cell. Therefore, pH readings of both acid cell and water cell were then acquired at a regular time interval for at least 90 min or longer if possible. All measurements were carried-out without stirring under quiescent conditions.

3.2. pH measuring process

(a) At the beginning of the experiment, the pH of both the acid cell and water cell are measured.
(b) Once the experiment is started, the measurement of pH is done at a regular interval (every 2–5 min) of time.
(c) The experiment is terminated after recording sufficient readings.
(d) The final value of pH in each cell (acid and water) is recorded.
(e) The concentration of protons is obtained using the relation: $[H^+] = 10^{-pH}$.

3.3. Measurement of proton transfer

To ensure protons are passing from acid cell to the water cell, initial proton conductivity tests were performed by measuring the pH at each cell for a long time period without placing any membrane. In principle, the pH of the acid cell should increase due to the loss of protons while the pH of the water cell should decrease due to receiving of protons. Initial test confirms the change in pH at each of the cells indicating that protons are migrated from acid cell to the water cell. Next, keeping the same initial concentration of protons in both the acid and water cells, commercial proton exchange membrane Nafion® [6] and several prototype in-house SAS (**s**tyrene–**a**crylonitrile–vinyl**s**ulfate) membranes were experimented using the same experimental set-up and experimental conditions. The membrane is placed between two-sided PEM holders as shown in Fig. 2. The pH and temperatures of both cells are recorded during entire experimentation at a regular time interval for a period of at least 90 min or longer wherever possible.

4. Results and discussions

To validate the theoretical model to measure membrane resistance to protons flow, according to Eq. (22) to determine C_0 and C_f, we conducted experiment based on two-cell model developed here. Initial proton transfer measurement is conducted using the apparatus set-up and procedures mentioned above. Fig. 3 represents the change of pH in water cell as a function of time without placing membrane between the two cells in order to test diffusion rate of protons (conduction of protons). Fig. 3 shows a complete profile of change of pH in the water cell which clearly displays three distinct phases – an *induction phase* representing the time taken for the acid to diffuse into the de-ionized water to release protons up to the moment of time to start transfer of protons from acid cell to water cell i.e. total time taken to gain first proton into the water cell; a *proton transfer phase* wherein protons started passing rapidly into the water cell – lowering the pH of the water cell, and an *equilibrium phase* wherein the pH of the initially water-only cell was lowered approximately to that of the initially acidified cell. The *proton transfer phase* is used to determine the concentration of protons (i.e. total amount of protons transferred) into the water cell per minute and the time from initiation of proton transfer into the initially water-only cell till attainment of the equilibrium pH between the two cells. In Fig. 3, the curve consists of three distinct segments for the rate of change of pH as a function of time: an initial slightly negative slope in *induction phase*, a greater negative slope in *proton transfer phase*, and finally a slightly negative slope in *equilibrium phase*. We divided the profile of pH obtained in Fig. 3 into three separate curves, one for each region of different slope, and a linear regression line is fitted to each curve segment with corresponding linear equations. Let the regression lines be

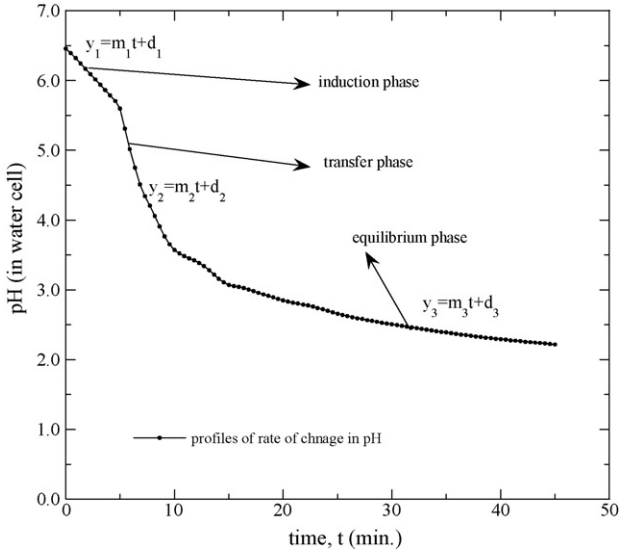

Fig. 3. Experimental results for the change of pH in water cell as a function of time with no membrane to determine the rate of diffusion of protons. Linear regression equations at each of the three distinct phases: induction phase, transfer phase and equilibrium phase, are shown in the onset. Slope of the curves indicate the rate of change of pH in each phase.

$$y_1 = m_1 t + d_1, \tag{24}$$

$$y_2 = m_2 t + d_2, \tag{25}$$

and

$$y_3 = m_3 t + d_3, \tag{26}$$

respectively, in three phase regions. Here, slopes m_1, m_2, and m_3 represent the rate of change of pH in water cell at each of the three distinct phases; *induction phase*, *transfer phase* and *equilibrium phase*, respectively. We can now calculate the concentration of protons at each of the phases via the relation:

$$\text{concentration of protons, } [\mathrm{H}^+] = 10^{-\mathrm{pH}}. \tag{27}$$

The strongly negative slope curve, in *transfer phase*, represents the maximum rate of proton transfer per minute and it can be obtained by using Eqs. (25) and (27). The two intersections of the three curves given in Eqs. (24)–(26) will provide the indication of transfer phase slope start and end time. Thus, we can calculate slope start time, induction time, as:

$$t_1 = \frac{d_2 - d_1}{m_1 - m_2}, \tag{28}$$

and the slope end time, equilibrium time, as:

$$t_2 = \frac{d_3 - d_2}{m_2 - m_3}. \tag{29}$$

To test the resistance of the proton exchange membrane, we placed the membrane between the two cells as shown in Fig. 2 and followed the procedures discussed in Sections 3.1–3.3. Keeping the same initial concentration of protons in the acid and water cells, widely used Nafion® [6] membrane and several prototypes in-house SAS membranes were examined using the same experimental set-up and conditions. Fig. 4 represents the rate of change of pH in water cell for different membranes tested here as a function of time. As mentioned above, since we maintained same initial concentrations of protons in the cells at the time of

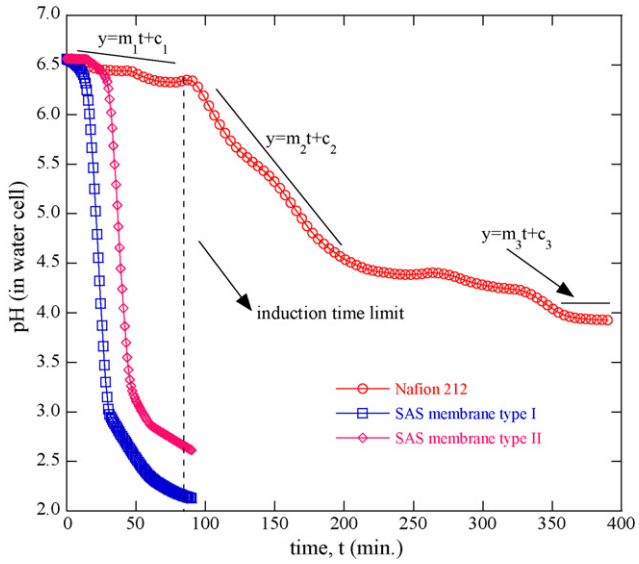

Fig. 4. Experimental results for the change of pH in water cell as a function of time with different membranes. Linear regression equations at each of the three distinct phases: induction phase, transfer phase and equilibrium phase, are shown in the onset. Slope of the curves indicate the rate of change of pH in each phase.

starting experiment for each of the membrane case, the initial pH was same for each case as can be seen from Fig. 4. In Fig. 4, we can see that the variations of three distinct phases for each of membranes; induction phase, transfer phase and equilibrium phase, as a function of time. It is due to the resistance of each membrane offered to the protons flow while it passes through the membrane. From Fig. 4, we can see clearly that the induction time varies for different membranes. Induction time has great impact on power supply from fuel cell during start up [2]. We calculated the rate of change (slope) of pH profiles for each of the tested membrane, using Eqs. (24)–(26), whose pH profiles in water cell is displayed in Fig. 4. Fig. 5 shows the rate of change of pH profiles in water cell obtained in Fig. 4. In Fig. 5, we can see that a steady constant slope at the induction phase, a significant slope variations in the transfer phase as protons started migration from acid cell to water cell to equilibrate the negative gradient created in the water cell, and finally a steady constant slope in the equilibrium phase which signals the attainment of pseudo-equilibrium in slopes between the acid cell and the water cell. These characteristics of slopes of pH profiles in water cell ascertain that how the proton conduction is taking place between the two cells.

From Fig. 5, we see that the very sharp decrease in slopes for both of the SAS membranes throughout the transfer phase as compared to Nafion® 212 membrane. Using the rate of change of pH in water cell in Fig. 5 and the relation given in Eq. (27) we calculated moles of protons migrated across the membrane and obtain the accurate concentration of protons per minute for each of the membranes. Fig. 6 represents the concentration profiles of protons flow as a function of time in water cell for various membranes obtained experimentally by placing membrane between the two test cells and the corresponding results obtained using the theoretical model, Eq. (22). For theoretical calculation, we used values of C_0 and C_f obtained experimentally through the rate of change of pH as shown in Fig. 5. In Fig. 6, experimental results and the theoretical results are indicated in parentheses. We can see an excellent agreement between the experimental and theoretical profiles of protons flow (see Fig. 6) in all of the three distinct phases – induction phase, transfer phase and equilibrium phase. The peak of the protons flow profiles represents the maximum rate of protons transfer. Among the profiles of protons flow for different membranes, SAS type 1 PEM has the highest peak and Nafion® 212 has the lowest peak, as can be seen from Fig. 6. It means that the SAS type 1 PEM able to transfer maximum number of protons at a moment of time than the Nafion® 212 membrane. Comparing results presented

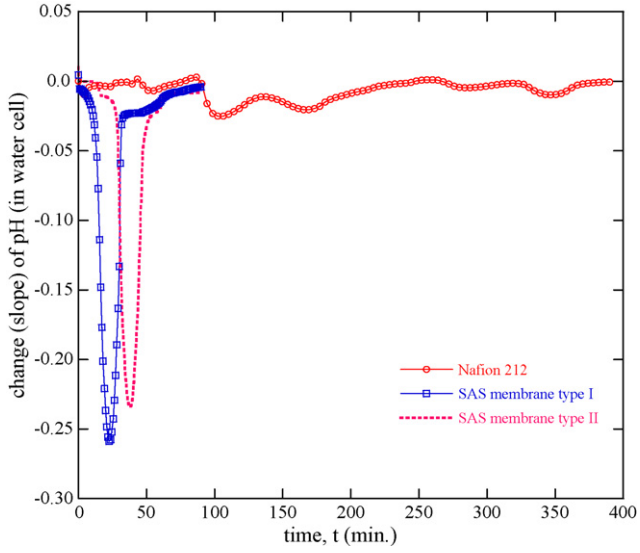

Fig. 5. Slopes of pH profiles in water cell as a function of time with different membranes. SAS membranes show very sharp decrease of slopes in the transfer phase as compared to Nafion® 212 membrane.

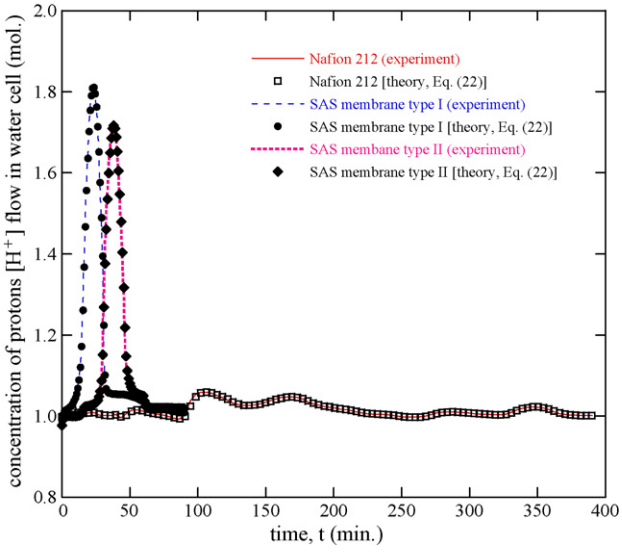

Fig. 6. Concentration profiles of protons flow in water cell as a function of time with different membranes. Symbols represent theoretical model predictions, Eq. (22). Solid-, dashed- and dotted-lines represent experimental results for different membranes.

Table 1
Comparison of proton transfer capacity and time required for protons to cross the membrane

Membrane type	Maximum protons transfer capacity (mol min^{-1})		Average protons transfer capacity (mol min^{-1})		Minimum time required for protons to cross the membrane (min mol^{-1})		Average time required for protons to cross the membrane (min mol^{-1})	
	Experiment	Theory [Eq. (22)]	Experiment	Theory [Eq. (22)]	Experiment	Theory [Eq. (22)]	Experiment	Theory [Eq. (22)]
Nafion® 212	1. 0593	1.0590	1. 0321	1.0321	0.9440	0.9443	0.9689	0.9689
SAS type I	1.8140	1.8121	1.7632	1.7631	0.5513	0.5518	0.5671	0.5672
SAS type II	1.7174	1.7166	1.6707	1.6707	0.5823	0.5825	0.5985	0.5986

Both experimental and theoretical results are presented.

Table 2
Comparison of induction time and relative resistance among membranes examined

Membrane type	Induction time (time required to start transfer proton) [Eq. (28)]	Minimum relative membrane resistance		Average relative membrane resistance		Rank of membrane based on low to high relative resistance
		Experiment	Theory [Eq. (23)]	Experiment	Theory [Eq. (23)]	
Nafion® 212	87.6045	1.71	1.71	1.76	1.76	SAS type I
SAS type I	15.0915	1	1	1.03	1.03	SAS type II
SAS type II	29.9235	1.06	1.06	1.09	1.09	Nafion® 212

Both experimental and theoretical results are presented.

in Fig. 6, we see that both of the SAS type PEMs are able to transfer higher number of protons at a moment of time than the commercial membrane Nafion® 212.

To determine the relative resistance among membranes, we calculated the proton transfer capacity and time required for each individual membrane to allow a specific amount of protons to pass through it. Table 1 represents both experimental and theoretical results of maximum and average proton transfer capacity as well as minimum and average time required for each of the membranes examined here. Maximum proton transfer capacity is determined using the highest peak slope shown in Fig. 6. On the other hand, average proton transfer capacity is calculated using the average slope in the entire transfer phase of protons concentration profiles displayed in Fig. 6. We then multiply the proton transfer capacity by 6.02×10^{23} (Avogadro number) to obtain the exact number of protons transferred through the membrane per minute. The values thus obtained can then be inverted to obtain time required per mole of protons and time required per proton, respectively, to pass through the membrane. We can see from Table 1 that the experimental results for different quantities agree well with the corresponding theoretical predictions. Comparing results among different membranes it can be seen that the SAS type membranes have higher protons transfer capacity, for both the maximum and average, than the peer Nafion® 212 membrane. SAS type membranes also took less time to allow a specific amount of protons to pass through it. Using the calculated results in Table 1, we calculated the induction time and relative resistance of the membranes, which is presented in Table 2. The induction time and relative resistance of membranes are calculated according to Eqs. (28) and (23), respectively. Comparing calculated results in Table 2, we can see that the SAS type I membrane took the lowest time and Nafion® 212 membrane required highest time to start of transfer of proton. The SAS type I membrane started proton transfer within as little as 16 min whereas Nafion® 212 did not begin to transfer protons even after 87 min. For the case of relative resistance, we can see that Nafion® 212 membrane has 71% higher resistance compared to SAS type I membrane. Once again, for determining relative resistance among membranes, the experimental results are in excellent agreement with the results obtained from theoretical model as can be seen from Table 2. Based on the low to high relative resistance we can rank among membranes. As per our tested membranes, SAS type I has the rank 1 and Nafion® 212 has rank 3. Thus, using the developed two-cell model and simple experimental set-up described here, we can measure relative resistance of membranes at the time of manufacturing.

5. Conclusions

A corrected version of two-cell model [1] for measuring the resistance offered by the proton exchange membrane to protons flow has been developed theoretically and validated experimentally. Detailed experimental set-up to validate the theoretical model has also been described. According to the theory developed here, the resistance of the proton exchange membrane is obtained in terms of the time required by the membrane to permit a certain number of protons to pass through it. A simple second order differential equation describes the entire process completely. Maintaining same experimental set-up, initial conditions and assuming steady state flow condition for entire duration of the experiment, the proton exchange membrane resistance can be determined by setting the concentration of protons in water cell, $C_w(t)$, to a constant as per Eq. (22). Comparison of the values of resistance for different membranes thus obtained will give an idea of the membrane which functions most efficiently in terms of proton transfer capacity and resistivity. The results for three different types of proton exchange membranes examined in this study show that the theoretical model predictions are in an excellent agreement with the experimental observations. Since electrolyte resistance is one of the key performance drivers for

the advancement of fuel cell technology, this investigation may open up a route to commercially fabricate a simple device to measure membrane resistance during efficient membrane manufacturing for energy applications.

Acknowledgement

This work is accomplished under the funding support provided by the U.S. Department of Energy (DOE) grant award number GO86056.

References

[1] B.V. Babu, N. Nair, J. Energy Edu. Sci. Technol. 13 (2004) 13–20.
[2] J. Larminie, A. Dicks, Fuel Cell Systems Explained, John Wiley & Sons, New York, 2000.
[3] A.J. Bard, L.R. Faulkner, Electrochemical Methods: Fundamentals and Applications, John Wiley &Sons, New York, 2001.
[4] US Department of Energy: Hydrogen, Fuel cells and Infrastructure Technologies Program (2006). (http://www1.eere.energy.gov/hydrogenandfuelcells/fuelcells).
[5] Y. Sugaya, M. Fukui, Y. Aoki, US Patent no. 6,569,301 (2001).
[6] Nafion®, E.I. DuPont de Nemours and Company, USA.
[7] T.D. Gierke, G.E. Munn, F.C. Wilson, J. Polym. Sci.: Polym. Phys. Ed. 19 (1981) 1687.
[8] A.J. Appleby, F.R. Foulkes, Fuel Cell Handbook, Van Nostrand Reinhold, New York, 1989.
[9] Achieving Accurate and Reliable Resistance Measurements in Low Power and Low Voltage Applications, Keithley Instruments white paper, 2004.
[10] M. Smith, K. Cooper, D. Johnson, L. Scribner, Fuel Cell Magazine, Webcom Communications Corp., 2005, April/May issue.
[11] T.A. Zawodzinski, T.E. Springer, F.A. Uribe, S. Gottesfeld, J. Solid State Ionics 60 (1993) 199.
[12] R. Treybal, Mass Transfer Operations, McGraw-Hill, Singapore, 1980.
[13] H.C. Edwards, D.E. Penney, Differential Equations: Computing and Modeling, third ed., Prentice Hall, NJ, 2003.